

Surface induced disorder in body-centered-cubic alloys

F. F. Haas, F. Schmid[‡], K. Binder

Institut für Physik, Universität Mainz, D-55099 Mainz, Germany

‡ Max-Planck-Institut für Polymerforschung, Ackermannweg 10, D-55021 Mainz, Germany

We present Monte Carlo simulations of surface induced disordering in a model of a binary alloy on a bcc lattice which undergoes a first order bulk transition from the ordered DO3 phase to the disordered A2 phase. The data are analyzed in terms of an effective interface Hamiltonian for a system with several order parameters in the framework of the linear renormalization approach due to Brézin, Halperin and Leibler. We show that the model provides a good description of the system in the vicinity of the interface. In particular, we recover the logarithmic divergence of the thickness of the disordered layer as the bulk transition is approached, we calculate the critical behavior of the maxima of the layer susceptibilities, and demonstrate that it is in reasonable agreement with the simulation data. Directly at the (110) surface, the theory predicts that all order parameters vanish continuously at the surface with a nonuniversal, but common critical exponent β_1 . However, we find different exponents β_1 for the order parameter (ψ_2, ψ_3) of the DO3 phase and the order parameter ψ_1 of the B2 phase. Using the effective interface model, we derive the finite size scaling function for the surface order parameter and show that the theory accounts well for the finite size behavior of (ψ_2, ψ_3) , but not for that of ψ_1 . The situation is even more complicated in the neighborhood of the (100) surface, due to the presence of an ordering field which couples to ψ_1 .

I. INTRODUCTION

First order phase transitions in the bulk of systems can drive a variety of interesting wetting phenomena at their surfaces and interfaces. They have attracted much attention over many years [1], and are still very actively investigated [2]. Prominent examples are the wetting of a liquid on a solid substrate at liquid-vapour coexistence, or the wetting of one component of a binary fluid below the demixing temperature on the walls of a container. These systems are representatives of a generic situation, which has been studied in particular detail: Three phases coexist, substrate, liquid and vapour. The substrate acts as inert “spectator” which basically provides the “boundary conditions” for the liquid-vapour system. The liquid-vapour transition can be described by a single order parameter (*e.g.*, the density), which can take two equilibrium bulk values at coexistence (the liquid density or the gas density). Obviously, the liquid phase will only wet the substrate if it is preferentially adsorbed by the latter. As one approaches the liquid-vapour coexistence from the vapour side, different scenarios are possible, depending on the substrate interactions and on the temperature: Either the liquid film covering the substrate remains microscopic at coexistence (“partial wetting”), or it grows macroscopically thick (“complete wetting”). The transition from partial to complete wetting can be first order or continuous (“critical wetting”). Since critical wetting is only expected on certain substrates at a specific temperature, it is rather difficult to observe experimentally (An experimental observation of critical wetting with long range forces has been reported in [3], and with short range forces in [4]).

Wetting phenomena are also present in alloys which undergo a discontinuous order-disorder transition in the bulk [5,6]. In many cases, surfaces are neutral with re-

spect to the symmetry of the ordered phase, but reduce the degree of ordering due to the reduced number of interacting neighbors. The surfaces can thus be wetted by a layer of disordered alloy, *i.e.*, “surface induced disorder” (SID) occurs [7,8]. The situation is reminiscent of liquid-vapour wetting; however, the underlying symmetry in the system restricts the possible wetting scenarios significantly.

We shall illustrate this for systems with purely short range interactions: We consider a Landau free energy functional of the form

$$\mathcal{F}\{\mathbf{m}\} = \int d\vec{r} \int_0^\infty dz \left\{ \frac{g}{2} (\nabla \mathbf{m})^2 + f_b(\mathbf{m}(\vec{r}, z)) \right\} + \int d\vec{r} f_s(\mathbf{m}(\vec{r}, z=0)). \quad (1)$$

Here the vector \mathbf{m} subsumes the relevant order parameters, the z -axis is taken to be perpendicular to the surface, and $d\vec{r}$ integrates over the remaining spatial dimensions. The offset of the bulk free energy density $f_b(\mathbf{m})$ is chosen such that $f_b(\mathbf{m}_b) = 0$ in the bulk. The surface contribution $f_s(\mathbf{m})$ accounts for the influence of the surface on the order parameter, *i.e.*, the preferential adsorption of one phase or in the case of SID the disordering effect. In mean field approximation, the functional (1) is minimized by the bulk equation

$$g \frac{d^2 m_i}{dz^2} = \partial_i f_b(\mathbf{m}), \quad (2)$$

which describes the motion of a classical particle of mass g in the external potential $(-f_b(\mathbf{m}))$, subject to the boundary condition at $z = 0$

$$g \frac{dm_i}{dz} = -\partial_i f_s(\mathbf{m}) \quad \text{with} \quad \left| g \frac{d\mathbf{m}}{dz} \right| = \sqrt{2g f_b(\mathbf{m})} \quad (3)$$

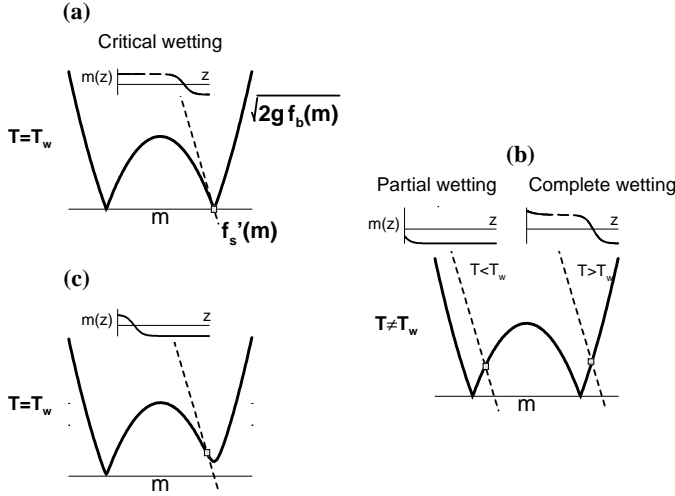


FIG. 1. Cahn construction (schematic) for a second order wetting transition: (a) Critical wetting, (b) Partial and complete wetting, (c) Off bulk coexistence, approaching critical wetting. Insets show the corresponding order parameter profiles. See text for more explanation.

If the order parameter has just one component, this equation can be solved graphically by the Cahn construction [9]. This is illustrated in Fig. 1 for the case of a continuous wetting transition. The corresponding order parameter profiles are shown as insets. Complete wetting is encountered if $f'_s(m)$ crosses $\sqrt{2gf_b}$ at the outer side of the minimum corresponding to the adsorbed phase. Partial wetting is found if the crossing point is located between the two minima (Fig. 1b). Critical wetting connects the two regimes, *i.e.*, $f'_s(m)$ crosses $\sqrt{2gf_b}$ right at the adsorbed phase minimum of f_b (Fig. 1a). Fig. 1c shows a case where the system is off bulk coexistence.

Now, let us consider the case of surface induced disorder. Here, several equivalent ordered phases exist, and the ordered state breaks a symmetry. For neutral surfaces which do not discriminate between the ordered phases, f_b and f_s have the same symmetry. This implies that f_s is extremal in the disordered phase ($\mathbf{m} = 0$), *i.e.*, $|\partial f_s|$ is zero at $\mathbf{m} = 0$ and thus crosses $\sqrt{2gf_b}$ at $\mathbf{m} = 0$

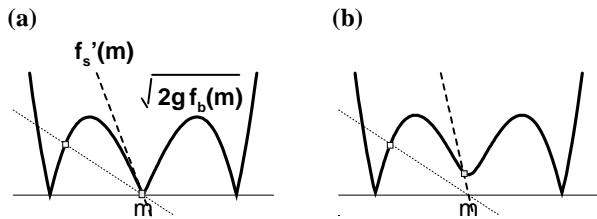


FIG. 2. Cahn construction (schematic) for surface induced disorder in a system with a one-component order parameter m (a) at bulk coexistence and (b) off bulk coexistence. Dashed line shows surface term $f'_s(m)$ for critical wetting, dotted line for partial wetting.

(Fig. 2). Comparing that with the scenario sketched above (Fig. 1), we find that surface induced disordering corresponds to either partial or critical wetting [6] – the symmetry of the surface interactions excludes the possibility of complete wetting [10]. The off-coexistence situation (Fig. 2b)) resembles that in Fig. 1c).

Alloys which exhibit surface induced disorder thus seem particularly suited to study critical wetting. Unfortunately, the simplification due to the symmetry of the system often goes along with severe complications in other respect: Usually, one has to deal with a number of order parameters and other coupled fields, which interact in a way that may not always be transparent. If the surface under consideration does not have the symmetry of the bulk lattice with respect to the ordered phases, the interplay of order parameters and surface segregation creates effective ordering surface fields [11–14], which may affect the critical behavior at the surface [14,15]. In the case of a one component order parameter, such a field drives the system from critical wetting to partial wetting. When several order parameters are involved, this is not necessarily the case [16–18]. More subtle effects can lead to surface order even at fully symmetric surfaces [19–21].

Experimentally, surface induced disorder has been investigated at the (100) surface of Cu_3Au [22–25]. A number of studies have provided evidence that the order parameter right at the surface vanishes continuously as the bulk transition is approached [22–24], and established the relation with the existence of a disordered surface layer of growing thickness [25]. The related case of “interface induced disorder” has been studied among other in Cu-Pd , where the width of anti-phase boundaries was shown to diverge logarithmically as the temperature of the transition to the disordered phase was approached from below [26].

The first simulation studies of surface induced disorder in different systems have reproduced the continuous decrease of the surface order parameter at the bulk first order transition [27,18,16], and the logarithmic growth of a disordered layer near the surface [16]. A detailed study of surface induced disorder at the (111) surface of CuAu has been published recently by Schweika *et al* [28]. The critical behavior of various quantities has been analyzed, and critical exponents were found which agree well with the theory of critical wetting. Most notably, Schweika *et al* observe nonuniversal exponents, as predicted by renormalization group theories of wetting phenomena [30,31]. In contrast, Monte Carlo simulations of critical wetting in a simple Ising model have given results which were more consistent with mean field exponents [29]. This latter finding has intrigued theorists for some time, and a number of theories have been put forward to account for the unexpected lack of fluctuation effects [32–34]. The nonuniversality of the exponents observed by Schweika *et al* seems to indicate that the fluctuations are restored in the case of SID. Alternatively, it may also stem from a competition of different length scales associated with the local order parameter and the local com-

position [17,18,35].

In the present work, we study surfaces of a bcc-based alloy close to the first order transition from the ordered DO_3 phase to the disordered phase. Our work is thus closely related to that of Schweika *et al.* It differs in that the order parameter structure in the bcc case is much more complex than in the fcc-alloy: Whereas only one (three dimensional) order parameter drives the transition considered by Schweika *et al.*, we have to deal with two qualitatively different order parameters, which are entangled with each other in a rather intriguing way. In fact, we shall see that one of them behaves as expected from the theory of critical wetting, whereas the other exhibits different critical exponents, which do not fit into the current picture.

A similar system has been investigated some time ago by Helbing *et al.* [16]. The systems studied there were rather small, and a detailed analysis of the critical behavior was not possible. Helbing *et al.* report evidence for the presence of a logarithmically growing disordered layer at the (100)-surface as phase coexistence was approached. In retrospect, this result seems surprising, since the (100) surface breaks the symmetry with respect to one of the order parameters, and we know nowadays that this nucleates an ordering surface field. In order to elucidate the influence of this ordering field in more detail, we have thus considered both the (110) surface, which has the full symmetry of the bulk lattice, and the (100) surface.

Our paper is organized as follows: In the next section, we provide some theoretical background on the theory of wetting in systems with several order parameters. Section III is devoted to some general remarks on order-disorder transitions in bcc-alloys, and to the presentation of the model and the simulation method. Our results are discussed in section IV. We summarize and conclude in section V.

II. EFFECTIVE INTERFACE THEORY OF SURFACE INDUCED DISORDER

A. General considerations

We have already sketched one of the popular mean field approaches to wetting problems in the introduction. Since the bulk of the system is not critical, one can expect fluctuations to be negligible for the most part. Only the fluctuations of the local position $l(\vec{r})$ of the interface between the growing surface layer and the bulk phase remain important [36]. As the interface moves into the bulk, capillary wave excursions of larger and larger wavelengths become possible. These introduce long-range correlations parallel to the surface, characterized by a correlation length ξ_{\parallel} which diverges at wetting.

In light of these considerations, fluctuation analyses often replace the Landau free energy functional (1) by an effective interface Hamiltonian [30,36,37]

$$\mathcal{H}\{l\}/k_B T = \int d\vec{r} \left\{ \frac{1}{8\pi\omega} (\nabla l)^2 + V_0(l) \right\}. \quad (4)$$

Here all lengths are given in units of the bulk correlation length ξ_b in the phase adsorbed at the surface, the parameter ω is the dimensionless inverse of the interfacial tension σ

$$\omega = k_B T / 4\pi\sigma\xi_b^2, \quad (5)$$

and the potential $V_0(l)$ describes effective interactions between the interface and the surface. The wetting transition is thus identified with a depinning transition of the interface from the surface.

In the linearized theory, the partition function of the Hamiltonian (4) is approximated by

$$\mathcal{Z} \approx \int \mathcal{D}\{l\} e^{-\int d\vec{r} (\nabla l)^2 / 8\pi\omega} \left[1 + \int d\vec{r} V_0(l) \right]. \quad (6)$$

It is convenient to switch from the real space \vec{r} to the Fourier space \vec{q} . The integration over short wavelength fluctuations with wavevector $|\vec{q}| > \lambda^{-1}$, where λ is arbitrary, is then straightforward: One separates l into a short wavelength part $\hat{l}(\vec{q}) = l(\vec{q}) \theta(q - \lambda^{-1})$ and a long wavelength part $\bar{l} = l - \hat{l}$, and exploits the relation $V_0(\bar{l} + x) = \exp[x d/dl] V_0(\bar{l})$, to obtain the unrescaled coarse grained potential [38]

$$\begin{aligned} \bar{V}_{\lambda}(\bar{l}) &= \int \mathcal{D}\{\hat{l}\} \exp \left[-\frac{1}{4\pi^2} \int d\vec{q} \left\{ \frac{|\vec{q}\hat{l}|^2}{8\pi\omega} + \hat{l} \frac{d}{dl} \right\} \right] V_0(\bar{l}) \\ &= \exp \left[\frac{\xi_{\perp,\lambda}^2}{2} \left(\frac{d}{dl} \right)^2 \right] V_{\lambda}(\bar{l}) \end{aligned} \quad (7)$$

$$\text{with } \xi_{\perp,\lambda}^2 = \frac{\omega}{\pi} \int_{q>1/\lambda}^{1/\Lambda} d\vec{q} \frac{1}{q^2} = 2\omega \ln(\lambda/\Lambda), \quad (8)$$

where Λ is a microscopic cutoff length. After rescaling $\vec{r} \rightarrow \vec{r}/\lambda$, $\bar{V}_{\lambda}(l) \rightarrow V_{\lambda}(l) = \lambda^{d-1} \bar{V}_{\lambda}(\bar{l}\lambda^{\zeta})$, and noting that the roughness exponent ζ is zero for capillary waves in $d = 3$ dimensions, this can be rewritten as

$$V_{\lambda}(l) = \frac{\lambda^2}{\sqrt{2\pi\xi_{\perp,\lambda}^2}} \int dh e^{-h^2/2\xi_{\perp,\lambda}^2} V_0(l+h). \quad (9)$$

Renormalizing the potential $V_0(l)$ thus amounts to convoluting it with a Gaussian of width $\xi_{\perp,\lambda}^2$ [30], which is the width of a free interface on the length scale λ parallel to the interface. In the case of a bound interface, a natural choice for λ is ξ_{\parallel} , the parallel correlation length of the interface. Since the remaining fluctuations after the renormalization should be small on this length scale, the procedure can be made self consistent by equating ξ_{\parallel} with its mean field value

$$4\pi\omega \frac{d^2}{dl^2} V_{\lambda}(l) \Big|_{l=\langle l \rangle} = (\xi_{\parallel}/\lambda)^{-2} = 1 \quad \text{at } \lambda = \xi_{\parallel} \quad (10)$$

where the average position of the interface $\langle l \rangle$ is the position of the minimum of $V_{\lambda}(l)$. Note that the renormalized

free energy density per area ξ_{\parallel}^2 is of order unity. The singular part F_s of the total interface free energy thus scales like $F_s \propto \xi_{\parallel}^{-2}$. From the renormalized Hamiltonian (4),

$$\mathcal{H}_{\xi_{\parallel}}\{l\}/k_B T = \frac{1}{4\pi^2} \int_0^{\xi_{\parallel}/\Lambda} d\vec{q} \frac{1}{8\pi\omega} (q^2 + 1) |l(\vec{q})|^2 \quad (11)$$

we can now calculate the distribution probability to find the interface at a position h ,

$$P(h) = \langle \delta[h - l(0)] \rangle_{\mathcal{H}_{\xi_{\parallel}}} = \frac{1}{\sqrt{2\pi\xi_{\perp}}} e^{-h^2/2\xi_{\perp}^2}, \quad (12)$$

and the joint probability distribution that the interface is found at h and h' at two points separated by \vec{r} from each other.

$$\begin{aligned} P^{(2)}(h, h', \vec{r}) &= \langle \delta[h - l(0)] \delta[h' - l(\vec{r})] \rangle_{\mathcal{H}_{\xi_{\parallel}}} \\ &= \frac{1}{2\pi\sqrt{g(0)^2 - g(r)^2}} \\ &\times \exp \left[-\frac{(h - h')^2}{4(g(0) - g(r))} - \frac{(h + h')^2}{4(g(0) + g(r))} \right], \end{aligned} \quad (13)$$

where

$$g(r) = \langle l(0) l(\vec{r}) \rangle_{\mathcal{H}_{\xi_{\parallel}}} = \frac{\omega}{\pi} \int_0^{\xi_{\parallel}/\Lambda} \frac{d\vec{q}}{q^2 + 1} e^{i\vec{q}\vec{r}/\xi_{\parallel}} \quad (14)$$

is the height-height correlation function of the interface and

$$\xi_{\perp}^2 = g(0) \approx 2\omega \ln(\xi_{\parallel}/\Lambda). \quad (15)$$

An analogous expression has been derived by Bedeaux and Weeks for a free liquid-gas interface in a gravitational field [39]. In three dimensions, the height-height correlation function for $r \gg \Lambda$ and $\xi_{\parallel} \gg \Lambda$ is a Bessel function K ,

$$g(r) = 2\omega K_0(r/\xi_{\parallel}). \quad (16)$$

We assume that the average order parameter profile $\langle m(z) \rangle$ is given by the average over mean field order parameter profiles $m_{\text{bare}}(z - l)$, centered around the local interface positions l , which are distributed according to the distribution function $P(l)$.

$$\langle m(z) \rangle = \int dl P(l) m_{\text{bare}}(z - l) \quad (17)$$

The distribution functions $P(h)$ and $P^{(2)}(h, h', r)$ can then be used to calculate various characteristics of the profiles:

For example, the effective width of the order parameter profile, $W = 1/(2 \partial \langle m \rangle / \partial z)_{\langle l \rangle}$, is broadened by $P(h)$ and diverges according to [40,41]

$$W^2 \approx W_0^2 + \frac{\pi}{2} \xi_{\perp}^2 \quad (18)$$

where W_0 denotes the “intrinsic width” of the mean field profile, $W_0 = 1/(2 dm_{\text{bare}}/dz)|_{z=0}$.

Another quantity of interest is the layer-layer susceptibility, which describes the order parameter fluctuations at a given distance from the surface,

$$\chi_{zz} = \int d\vec{r} \left\{ \langle m(0)m(\vec{r}) \rangle_z - \langle m \rangle_z^2 \right\}. \quad (19)$$

Since it has the dimension of a square length, one deduces immediately that χ_{zz} scales like ξ_{\parallel}^2 in the interfacial region. For a more detailed analysis, we rewrite χ_{zz} as

$$\begin{aligned} \chi_{zz} &= \int d\vec{r} \int dh dh' m_{\text{bare}}(z - h) m_{\text{bare}}(z - h') \\ &\times \int d\vec{r} \{ P^{(2)}(h, h', r) - P(h) P(h') \}, \end{aligned} \quad (20)$$

expand the joint probability $P^{(2)}(h, h', r)$ in powers of $\Delta(r) = g(r)/\xi_{\perp}^2 = K_0(r/\xi_{\parallel})/\ln(\xi_{\parallel}/\Lambda)$,

$$\begin{aligned} P^{(2)}(h, h', r) &= P(h) P(h') \left\{ 1 + \frac{h h'}{\xi_{\perp}^2} \Delta(r) \right. \\ &\left. + \frac{1}{2} \left[1 - \frac{h^2 + h'^2}{\xi_{\perp}^2} + \frac{h^2 h'^2}{\xi_{\perp}^4} \right] \Delta(r)^2 + \dots \right\}, \end{aligned} \quad (21)$$

and recall $\int dr r K_0(r) = 1$ and $\int dr r K_0(r)^2 = 1/2$. If the intrinsic width of the profile $m_{\text{bare}}(z)$ is small compared to ξ_{\perp} , the intrinsic profile can be approximated by a simple step profile in the interfacial region, $m_{\text{bare}}(z) = m_b \theta(z)$, where m_b is the bulk order parameter. One then obtains

$$\begin{aligned} \chi_{zz} &= m_b^2 \xi_{\parallel}^2 e^{-(z - \langle l \rangle)^2 / \xi_{\perp}^2} \\ &\times \left(\frac{2\omega}{\xi_{\perp}^2} + \left(\frac{2\omega}{\xi_{\perp}^2} \right)^2 \frac{(z - \langle l \rangle)^2}{4\xi_{\perp}^4} + \dots \right). \end{aligned} \quad (22)$$

So far, these results are valid for infinite systems. The restriction to finite lateral dimension L affects the interface distribution $P(h)$ (12) in two ways: It introduces a lower cutoff ξ_{\parallel}/L in the integrals over \vec{q} (e.g., (14)), and the mean position of the interface (the zeroth mode) is no longer fixed at the minimum of the renormalized potential, but distributed according to $\exp[-L^2 V_{\xi_{\parallel}}(h)]$. The width of the distribution function $P(h)$ is now given by

$$\begin{aligned} \xi_{\perp}^2 &= \frac{\omega}{\pi} \int_{\xi_{\parallel}/L}^{\xi_{\parallel}/\Lambda} \frac{d\vec{q}}{q^2 + 1} + L^2 \frac{d^2 V_{\xi_{\parallel}}(h)}{dh^2} \Big|_{h=\langle l \rangle} \\ &= 2\omega \ln\left(\frac{\xi_{\parallel}}{\Lambda}\right) - \omega \ln\left(1 + \left(\frac{\xi_{\parallel}}{L}\right)^2\right) + 4\pi\omega \left(\frac{\xi_{\parallel}}{L}\right)^2. \end{aligned} \quad (23)$$

B. Bare and renormalized effective interface potential

We shall now apply these general considerations to a specific potential $V_0(l)$, designed to describe systems with

short range interactions and several order parameters and nonordering densities. Effective interface potentials for systems with two order parameters have been derived by Hauge [35] and Kroll and Gompper [17]. Their approach can readily be generalized to the case of arbitrary many order parameters and nonordering densities. We choose the coordinate system in the order parameter and density space $\{\mathbf{m}\}$ such that $\mathbf{m} = 0$ in the phase which wets the surface, and that the coordinate axes m_i point in the directions of the principal curvatures of the bulk free energy function $f_b(\mathbf{m})$. Close to this phase, f_b can then be approximated by the quadratic form

$$f_b(\mathbf{m}) = \frac{g}{2} \sum_i \frac{1}{\lambda_i^2} m_i^2 + \mu, \quad (24)$$

where μ is the field which drives the system from coexistence, and the λ_i have the dimension of a length. We number the coordinate axes i ($i \geq 0$) such that the λ_i are arranged in descending order. The largest of these dominates the correlations at large distances and is thus the correlation length ξ_b , *i.e.*, $\lambda_0 = \xi_b \equiv 1$ in our units. The surface contribution has the form

$$f_s(\mathbf{m}) = \sum_i h_{i,1} m_i + \frac{1}{2} \sum_{ij} c_{ij} m_i m_j. \quad (25)$$

Following Hauge and Kroll/Gompper, we now assume that the actual profile from the adsorbed phase to the bulk phase is close to the profile of a free interface between these two phases. Close to the surface region, we thus approximate the former by the test function

$$m_i(z) = v_i \exp(z - l)/\lambda_i \quad (26)$$

(at $z \ll l$), where l denotes the position of the effective interface. Inserting this into eqn. (1) with (24) and (25), we obtain the effective interface potential

$$V_0(l) = \sum_i a_i e^{-l/\lambda_i} + \sum_{ij} b_{ij} e^{-l(1/\lambda_i + 1/\lambda_j)} + \mu l \quad (27)$$

for $l \gg 0$, with $a_i = h_{i,1} v_i$ and $b_{ij} = \frac{1}{2}(c_{ij} - g\delta_{ij}/\lambda_i)v_i v_j$. This expression is of course only valid for large l . Notably, it fails at $l = 0$, since the true potential $V_0(l)$ must diverge there. We shall suppose that the leading term $b_{00} \equiv b$ in the second sum is positive and dominates over the more rapidly decaying terms, and disregard the latter in the following.

At $\omega = 0$ (or in mean field approximation), the interface is flat, and its position is given by the minimum of $V_0(l)$. At nonzero ω , the potential has to be renormalized as described in the previous section. Now the renormalization is straightforward if the fluctuations are sufficiently small that the interface position $\langle l \rangle$ at wetting is well in the asymptotic tail of the potential (weak fluctuation limit). According to a criterion introduced by Brézin, Halperin, and Leibler [30], this is true as long

as $\int_0^\infty dl e^{-(l-\langle l \rangle)^2/2\xi_\perp^2} V_0(l) \approx \int_{-\infty}^\infty dl e^{-(l-\langle l \rangle)^2/2\xi_\perp^2} V_0(l)$, *i.e.*,

$$2\xi_\perp^2 - \langle l \rangle < 0 \quad \text{and} \quad \xi_\perp^2/\lambda_i - \langle l \rangle < 0 \quad (28)$$

for all λ_i . For $\lambda_i > 1/2$, the first inequality enforces the second one. In a system with one order parameter, it leads to the well-known inequality $\omega < 1/2$ [30,31]. As we shall see shortly, this condition is also sufficient to ensure the validity of the weak fluctuation limit in a system with several order parameters. Since ω in our simulations turns out to be much smaller than $1/2$, we shall not discuss the other regimes in the present paper.

In the weak fluctuation limit, the renormalized potential takes the form

$$\frac{V_{\xi_\parallel}(l)}{\xi_\parallel^2} = \sum_{i:\lambda_i < 1/2} a_i e^{-l/\lambda_i} \left(\frac{\xi_\parallel}{\Lambda}\right)^{\omega/\lambda_i^2} + b \left(\frac{\xi_\parallel}{\Lambda}\right)^{4\omega} e^{-2l} + \mu l. \quad (29)$$

The cutoff parameter Λ is of the order of the correlation length, $\Lambda \approx \xi_b = 1$, and will be dropped hereafter.

C. Free energy scaling

Now our task is to determine ξ_\parallel self consistently by use of eqn. (10), which will yield the scaling behavior of the singular part of the surface free energy, $F_s \propto \xi_\parallel^{-2}$. Before generalizing to several order parameters, we shall briefly discuss the situation in a system with only one length scale λ_0 . The formal likeness of the more general theory with this often discussed special case can thus be highlighted. Moreover, many of the results derived for one order parameter carry over directly to the case of several order parameters.

In a system with one order parameter, the singular free energy has the scaling form

$$F_s \propto \xi_\parallel^{-2} = 8\pi\omega \mu f(\Phi_0), \quad (30)$$

where the scaling function $f(\Phi_0)$ depends on the dimensionless parameter

$$\Phi_0 = C_0 \mu^{(\omega-1)/2} a_0 \quad \text{with} \quad C_0 = \sqrt{(8\pi\omega)^\omega/2b}. \quad (31)$$

Depending on the value of Φ_0 , one can distinguish between different regimes:

$$\begin{aligned} \Phi_0 \gg 1: \quad & f(\Phi_0) = 1/2 g_1(2^\omega \Phi_0^{-2}) \\ & \text{with } g_1(x) \approx 1 + x - (2 + \omega)x^2 + \dots \\ & \text{(complete wetting)} \end{aligned} \quad (32)$$

$$\begin{aligned} |\Phi_0| \ll 1: \quad & f(\Phi_0) \approx 1 - \frac{1}{2}\Phi_0 + \frac{2 + \omega}{8}\Phi_0^2 + \dots \\ & \text{(critical wetting, field like)} \end{aligned} \quad (33)$$

$$\begin{aligned} \Phi_0 \ll -1 : f(\Phi_0) &= (\Phi_0^2/2)^{1/(1-\omega)} g_2((\Phi_0^2/2)^{-1/(1-\omega)}) \\ \text{with } g_2(x) &\approx 1 + \frac{3x}{2(1-\omega)} - \frac{(2+7\omega)x^2}{8(1-\omega)^2} + \dots \\ &\text{(partial wetting)} \end{aligned} \quad (34)$$

The point $\Phi_0 = 0$ is the critical wetting point. If one approaches this point from the partial wetting side $a_0 \rightarrow 0^-$ on the coexistence line $\mu = 0$, the parallel correlation length ξ_{\parallel} diverges with the well-known nonuniversal exponent

$$\xi_{\parallel} = (2\pi\omega/b)^{-1/2(1-\omega)} (-a_0)^{-1/(1-\omega)}, \quad (35)$$

and the distance between the average position of the interface and the surface diverges asymptotically like

$$\langle l \rangle \rightarrow -(1+2\omega)/(1+\omega) \ln(-a_0). \quad (36)$$

The relevant regime for most cases of surface induced disorder is however the critical wetting regime, where the critical wetting point is approached under a finite angle to the coexistence line in (a_0, μ) space. Here the parallel correlation length ξ_{\parallel} scales like

$$\xi_{\parallel} = \frac{1}{\sqrt{8\pi\omega}} \mu^{-\nu_{\parallel}} \quad \text{with} \quad \nu_{\parallel} = 1/2. \quad (37)$$

as μ approaches zero, the width of the interface diverges with

$$W^2 \rightarrow \frac{\pi}{2} \xi_{\perp}^2 = -\frac{\pi}{2} \omega \ln(\mu), \quad (38)$$

and its average position with

$$\langle l \rangle \approx -(\omega + 1/2) \ln(\mu). \quad (39)$$

These results can be used to derive the layer-bulk susceptibility of the order parameter in the interfacial region

$$\chi_{0,\langle l \rangle} = \left. \frac{\partial \langle m_0 \rangle}{\partial \mu} \right|_{\langle l \rangle} \propto - \left. \frac{\partial \langle m_0 \rangle}{\partial z} \right|_{\langle l \rangle} \frac{\partial \langle l \rangle}{\partial \mu} \propto \frac{1}{\mu \sqrt{\ln(\mu)}}. \quad (40)$$

In the step approximation $m_{0,\text{bare}}(z) = m_{0,b}\theta(z)$, the layer-bulk susceptibility in the interfacial region can be calculated in more detail:

$$\chi_{0,z} = \frac{m_{0,b}}{\sqrt{2\pi} \xi_{\perp} \mu} e^{-(z-\langle l \rangle)^2/2\xi_{\perp}^2} \left(\omega + \frac{1}{2} - \frac{z-\langle l \rangle}{2 \ln \mu} \right). \quad (41)$$

It has a slightly asymmetric peak of width ξ_{\perp} at $z = \langle l \rangle$, the height of which scales like $1/\mu$.

The layer-layer susceptibility could already be derived in the previous section. It also has a peak at the interface, which is however a factor of $\sqrt{2}$ narrower. Its height scales like

$$\chi_{\langle l \rangle \langle l \rangle} \propto \xi_{\parallel}^2 / \xi_{\perp}^2 \propto -1/(\mu \ln(\mu)). \quad (42)$$

Next we determine the critical behavior of the order parameter at the surface, $m_{0,1}$,

$$m_{0,1} \propto -\frac{\partial F_s}{\partial h_{0,1}} \propto -\frac{\partial \xi_{\parallel}^{-2}}{\partial a_0} \propto \mu^{\beta_{0,1}}, \quad \beta_{0,1} = \frac{1+\omega}{2} \quad (43)$$

It will prove useful to rederive the exponent $\beta_{0,1}$ in an alternative way: The surface order parameter in mean field theory is given by $m_{\text{bare}}(0) = m_b \exp(-l/\lambda_0)$. Averaging the profile according to eqn. (17) yields

$$m_{0,1} = m_b \langle e^{-l/\lambda_0} \rangle_{P(l)} = m_b e^{-\langle l \rangle / \lambda_0 + \xi_{\perp}^2 / 2\lambda_0^2}. \quad (44)$$

After inserting $\lambda_0 = 1$ and using eqns. (39) and (38), one recovers the power law of eqn. (43) with the same exponent $\beta_{0,1}$. The approach has the advantage that it allows for a straightforward calculation of finite size effects on surface critical behavior: We simply replace the expression (38) for ξ_{\perp} in the infinite system by eqn. (23) to obtain

$$m_{0,1} \propto m_b \mu^{\beta_{0,1}} \hat{M}_0(8\pi\omega \mu L^{1/\nu_{\parallel}}) \quad (45)$$

with the scaling function

$$\hat{M}_0(x) = \left(\frac{x}{x+1} \right)^{\omega/2} e^{2\pi\omega/x}. \quad (46)$$

We are now ready to generalize these results to the case of several order parameters and nonordering densities. Formally, the theory turns out to remain very similar. The self consistent determination of ξ_{\parallel} leads to a generalized version of the scaling form for the singular part of the surface free energy (30),

$$F_s \propto \xi_{\parallel}^{-2} = 8\pi\omega \mu f(\{\Phi_i\}), \quad (47)$$

where the scaling variables are

$$\Phi_i = C_i \mu^{(1-2\lambda_i)(1-\omega/\lambda_i)/2\lambda_i} a_i \quad (48)$$

$$\text{with} \quad C_i = (8\pi\omega)^{\omega/2\lambda_i^2 \cdot (2\lambda_i-1)} (2b)^{-1/2\lambda_i}.$$

As in the one-order parameter case, we have to distinguish between different regimes depending on the values of the scaling variables.

D. Symmetry preserving and symmetry breaking surfaces

Let us first assume that the effect of nonordering densities can be disregarded (*e.g.*, because the associated length scales are small, $\lambda_i < 1/2$), and consider the case of a symmetry preserving surface. No ordering surface fields are then present, *i.e.*, $a_i \propto h_i = 0$ for all contributions i . The system is thus in a “multicritical wetting regime”, where $|\Phi_i| \ll 1$ for all i , and the scaling function can be expanded as

$$f(\{\Phi_i\}) = 1 - \sum_i \Phi_i \frac{2\lambda_i - 1}{2\lambda_i^2} + \dots \quad (49)$$

The effective interface position $\langle l \rangle$, and the correlation length ξ_{\parallel} are given by eqns. (39) and (37) as in the case of normal critical wetting. Hence all the results related to interfacial properties, such as the interfacial width, the interfacial layer susceptibilities etc., remain unchanged. In particular, the criterion for the validity of the weak fluctuation limit is still $\omega < 1/2$ (from eqns. (28), (38) and (39)). The surface order parameters obey the power law

$$m_{i,1} \propto -\frac{\partial \xi_{\parallel}^{-2}}{\partial a_i} \propto \mu^{\beta_{i,1}}, \quad \beta_{i,1} = \frac{1}{2\lambda_i} + \frac{\omega}{2\lambda_i^2}(2\lambda_i - 1). \quad (50)$$

Following the lines of (44), one also obtains the finite size scaling function

$$\hat{M}_i(x) = \left(\frac{x}{x+1}\right)^{\omega/2\lambda_i^2} e^{2\pi\omega/x\lambda_i^2}. \quad (51)$$

A whole sequence of surface exponents is thus predicted, one for each order parameter. In practice, however, one hardly ever measures only one "pure" order parameter m_i . Instead, one expects to observe some combination of contributions with different exponents $\beta_{i,1}$, which will be dominated by the leading exponent $\beta_{0,1} = (\omega + 1)/2$ in the asymptotic limit $\mu \rightarrow 0$.

The situation changes when at least one of the a_i becomes nonzero at coexistence. This is the case, *e.g.*, at a symmetry breaking surface, where one or several surface fields become nonzero, or even at a symmetry preserving surface if the length scale associated with a nonordering density exceeds half the bulk correlation length, $\lambda_i > 1/2$.

Let $a_J e^{-l/\lambda_J}$ be the leading nonvanishing term in the potential (27). As one approaches coexistence, $\mu \rightarrow 0$, the scaling variable Φ_J increases and one eventually enters a regime $|\Phi_J| \gg 1$. For negative a_J , ($\Phi_J \ll -1$), the wetting becomes partial, *i.e.*, no surface induced disordering takes place. For positive a_J , ($\Phi_J \gg 1$), different scenarios are possible, depending on the sign and the amplitude of the higher order terms a_i , ($i > J$) in eqn. (29). If they are positive or sufficiently small, such that

$$|a_i a_J^{-\lambda_J/\lambda_i}| \ll 1, \quad (52)$$

the disordered phase wets the surface. The effective interface position $\langle l \rangle$ diverges asymptotically like

$$\langle l \rangle \approx -\lambda_J(1 + \omega/2\lambda_J^2) \ln(\mu), \quad (53)$$

the parallel correlation length scales like

$$\xi_{\parallel} = \sqrt{\lambda_J/4\pi\omega\mu}, \quad (54)$$

and the scaling function in eqn. (47) takes the form

$$f(\{\Phi_i\}) = \frac{1}{2\lambda_J} \left(1 + \sum_i \Phi_i \Phi_J^{-\lambda_J/\lambda_i} K_J(\lambda_i) + \frac{1}{2} \Phi_J^{-2\lambda_J} K_J\left(\frac{1}{2}\right) \right). \quad (55)$$

with

$$K_J(\lambda_i) = \frac{\lambda_J^{\lambda_J/\lambda_i}}{\lambda_i} \left(\frac{\lambda_J}{\lambda_i} - 1 \right) (2\lambda_J)^{\omega/2\lambda_i^2 \cdot (1-\lambda_i/\lambda_J)}.$$

According to eqn. (28), the weak fluctuation regime here is bounded by $\omega < 2\lambda_J^2$, thus encompassing the regime $\omega < 1/2$.

The criterion (52) is motivated as follows: If one of the higher order a_i is negative and large, the interface potential $V_{\xi_{\parallel}}(l)$ may exhibit a second minimum closer to the surface, which competes with the minimum at large l and may prevent the formation of an asymptotically diverging wetting layer. The inspection of the free energy scaling function (55) reveals that the transition to such a partial wetting regime is appropriately described in terms of the combined scaling variable

$$\tilde{\Phi}_{i,J} = \Phi_i \Phi_J^{-\lambda_J/\lambda_i} \propto a_i a_J^{-\lambda_J/\lambda_i} \mu^{(\lambda_J/\lambda_i - 1)(1 - \omega/(2\lambda_i\lambda_J))}.$$

This quantity has to be large at the point μ_0 where the one minimum of $V_{\xi_{\parallel}}(l)$ splits up in two. The condition (52) ensures that $\tilde{\Phi}_{i,J}$ is small for all μ .

The wetting is critical with respect to all order parameters m_i with length scales λ_i larger than λ_J . As coexistence is approached, they vanish at the surface according to the power law

$$m_{i,1} \propto -\frac{\partial \xi_{\parallel}^{-2}}{\partial a_i} \propto \mu^{\beta_{i,1}}, \quad \beta_{i,1} = \frac{\lambda_J}{\lambda_i} + \frac{\omega}{2\lambda_i^2} \left(\frac{\lambda_i}{\lambda_J} - 1 \right). \quad (56)$$

The finite size scaling function $\hat{M}_i(x)$ is again given by (51), with the scaling variable $x = 4\pi\omega\mu L^2/\lambda_J$. Note that the exponents $\beta_{i,1}$ are nonuniversal even in the mean field limit ($\omega = 0$). This remarkable effect has first been discovered by Hauge [35] and later studied by Kroll/Gompper in an fcc Ising antiferromagnet using a mean field approximation [17], Monte Carlo simulations, and a linear renormalization group study similar to the one presented here [18]. However, $\langle l \rangle$ in this work is taken from eqn. (36) rather than determined self consistently, hence the resulting critical exponents differ somewhat from those calculated here. As in the case of the symmetry preserving surface, a whole set of exponents is predicted by eqn. (56). In the asymptotic limit $\mu \rightarrow 0$, however, the surface behavior is expected to be governed by the leading exponent

$$\beta_{0,1} = \frac{\xi_b}{\lambda_J} + \frac{\omega}{2} \left(\frac{\xi_b}{\lambda_J} - 1 \right). \quad (57)$$

We have reinserted the bulk correlation length $\xi_b \equiv 1$ here.

Finally, we discuss the critical behavior of the surface susceptibilities. The corresponding critical exponents can be shown to obey simple scaling laws. In the case of the surface-bulk susceptibility, the relation follows trivially:

$$\chi_{i,1} \propto \frac{\partial m_{i,1}}{\partial \mu} \propto \mu^{-\gamma_{i,1}}, \quad \gamma_{i,1} = 1 - \beta_{i,1}. \quad (58)$$

In the case of the surface-surface susceptibility, it depends on the regime under consideration. In the "critical wetting regimes" discussed here, the free energy scaling function f can be expressed as a Taylor series in powers of the scaling variables Φ_i or $\tilde{\Phi}_{i,J}$, respectively, and one obtains

$$\chi_{i,11} \propto \frac{\partial m_{i,1}}{\partial h_{i,1}} \propto \mu \frac{\partial^2 f}{\partial a_i^2} \propto \mu^{-\gamma_{i,11}}, \quad \gamma_{i,11} = 1 - 2\beta_{i,1}. \quad (59)$$

The dominating exponents in the asymptotic limit are $\gamma_{0,1}$ and $\gamma_{0,11}$.

III. MODELING ORDER-DISORDER TRANSITION IN BCC-ALLOYS

Fig. 3 shows some typical structures of binary (AB) bcc-alloys (*e.g.*, FeAl [42]). It is useful to divide the bcc lattice into four fcc-sublattices a–d as indicated in the Figure. The phase transitions are then conveniently described in terms of a set of order parameters [43]

$$\begin{aligned} \psi_1 &= (c_a + c_b - c_c - c_d) \\ \psi_2 &= (c_a - c_b + c_c - c_d) \\ \psi_3 &= (c_a - c_b - c_c + c_d), \end{aligned} \quad (60)$$

where c_α denotes the composition on the sublattice α , *i.e.*, the average concentration of one component A there. In the disordered phase, all sublattice compositions are equal and these order parameters vanish. The B2 phase is characterized by nonzero ψ_1 , and the DO₃ phase in addition by nonzero $\psi_2 = \pm\psi_3$. By symmetry, physical quantities have to be invariant under sublattice exchanges $(a \leftrightarrow b)$, $(c \leftrightarrow d)$, and $(a,b) \leftrightarrow (c,d)$. The leading terms in a Landau expansion of the free energy F thus read

$$F = F_0 + A_1\psi_1^2 + A_2(\psi_2^2 + \psi_3^2) + B\psi_1\psi_2\psi_3 + C_1\psi_1^4 + C_2(\psi_2^4 + \psi_3^4) + C_3\psi_2^2\psi_3^2 + C_4\psi_1^2(\psi_2^2 + \psi_3^2), \quad (61)$$

We point out in particular the cubic term $B\psi_1\psi_2\psi_3$. It can be read in two ways. On the one hand, it describes how the B2-order influences the DO₃ order: The order parameter ψ_1 breaks the symmetry with respect to indi-

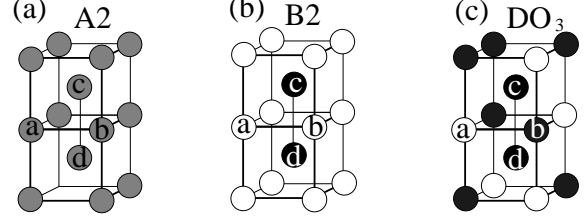


FIG. 3. bcc lattice with (a) disordered A2 structure (b) B2 structure, and (c) DO₃ structure. Also shown is the assignment of sublattices a,b,c,d.

vidual sign reversal of ψ_2 or ψ_3 and orients (ψ_2, ψ_3) such that $\psi_2 = -\text{sign}(B\psi_1)\psi_3$. Conversely, one can interpret the product $\psi_2\psi_3$ as an effective ordering field acting on ψ_1 . We shall come back to this point later.

At the presence of surfaces, the situation is even more complicated. First, we can always expect that one component enriches at the surface, since there are no symmetry arguments to prevent that. Even if no explicit surface field coupling to the total concentration c is applied, the component which is in excess with respect to the ideal stoichiometry of the bulk phase ((3:1) in the DO₃ phase) will segregate to the surface. Second, we have already mentioned that the Landau expansion of the surface free energy f_s depends on the orientation of the surface [11,14]. The (110) surface has the same symmetry with respect to sublattice exchanges as the bulk, hence the Landau expansion of the surface free energy must have the form (61). In case the order is sufficiently suppressed at the surface, one can thus hope to find classical surface induced disordering here. In the case of the (100) surface, the symmetry with respect to the exchange $(a,b) \leftrightarrow (c,d)$ is broken. The surface enrichment of one component then induces an effective ordering surface field, which couples to the order parameter ψ_1 [12]. Other ordering fields coupling to ψ_2 and ψ_3 are still forbidden by symmetry. The full spectrum of possible ordering surface fields is allowed in the case of the (111) surface.

In order to model these phase transitions, we consider an Ising model of spins $S_i = \pm 1$ on the bcc-lattice with antiferromagnetic interactions between up to next nearest neighbors,

$$\mathcal{H} = V \sum_{\langle ij \rangle} S_i S_j + \alpha V \sum_{\langle\langle ij \rangle\rangle} S_i S_j - H \sum_i S_i. \quad (62)$$

where the sum $\langle ij \rangle$ runs over nearest neighbour and $\langle\langle ij \rangle\rangle$ over next nearest neighbour pairs. Spins $S = +1$ represent A-atoms and $S = -1$ B-atoms, hence the concentration c of A is related to the average spin $\langle S \rangle$ via

$$c = (\langle S \rangle + 1)/2, \quad (63)$$

and the field H represents a chemical potential. The parameter $\alpha = 0.457$ is chosen such that the highest temperature which can still support a B2 phase is about twice

as high as the highest temperature of the DO_3 phase, like in the experimental phase diagram of FeAl. The phase diagram of our model is shown in Figure 4.

The surface simulations were performed in a $L \times L \times D$ geometry with periodic boundary conditions in the L direction and free boundary conditions in the D direction, varying D from 100 to 200 and L from 20 to 100. In order to handle systems of that size efficiently, we have developed [44] a multispin code [45], which allowed to store the configurations bitwise instead of byte-wise [46]. Our Monte Carlo runs had total lengths of up to $2 \cdot 10^6$ Monte Carlo sweeps.

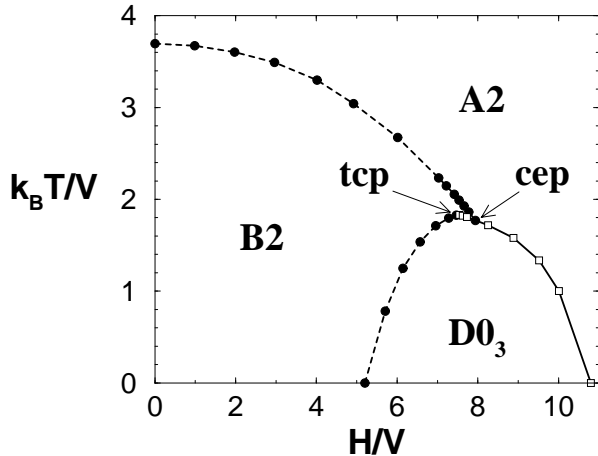


FIG. 4. Phase diagram of our model in the $T - H$ plane. Solid lines mark first order phase transitions, dashed lines second order phase transitions. Arrows indicate the positions of a critical end point (cep) and a tricritical point (tcp).

IV. SIMULATION RESULTS

We have studied (110) and (100) oriented surfaces at $T = 1 V/k_B$ close to the first order bulk transition between the ordered DO_3 phase and the disordered A2 phase. The exact bulk transition point was determined previously from bulk simulations by thermodynamic integration [47], $H_0/V = 10.00771(1)$ [44]. In the presence of such a high bulk field, the very top layer of a free (110) or (100) surface is completely filled with A particles, *i.e.*, Ising spins $S = 1$. Consequently, the order parameters ψ_α and the layer susceptibilities vanish there. In the following, we shall generally disregard this top layer and analyze the profiles starting from the second layer.

A. (110) Surfaces – DO_3 order

We begin with a detailed discussion of surface induced disordering at (110) surfaces, *i.e.*, surfaces with the full

symmetry of the bulk. Figure 5 shows profiles of the order parameter of DO_3 ordering per site

$$\psi_{23} = \sqrt{(\psi_2^2 + \psi_3^2)/2}. \quad (64)$$

One clearly sees how a disordered layer forms and grows in thickness as the bulk transition is approached. In order to extract an interface position $\langle l \rangle$ and an effective interfacial width W , we have fitted the profiles to a shifted tanh function

$$\psi_{23}(n) = \psi_{23}^{\text{bulk}} \left(1 + \exp \left[-2(z - \langle l \rangle)/W \right] \right)^{-1}. \quad (65)$$

The results are shown in Figs. 6 and 7. Sufficiently close to the bulk transition, at $(H_0 - H)/V < 0.005$, the data are consistent with the logarithmic divergence predicted by eqns. (39) and (18). Intuitively, one would expect that an effective interface theory is only applicable if $l > W$,

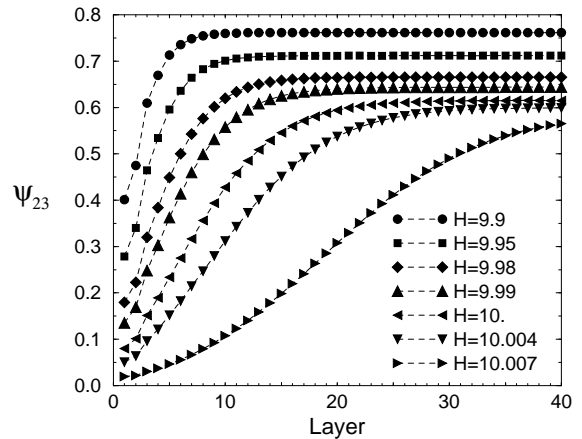


FIG. 5. Profiles of ψ_{23} near a (110) surface at temperature $T = 1 V/k_B$ for different fields H in units of V as indicated. The bulk transition is at $H_0/V = 10.00771(1)$. Zeroth (top) layer is not shown ($\psi_{23}(0) \equiv 0$, see text).

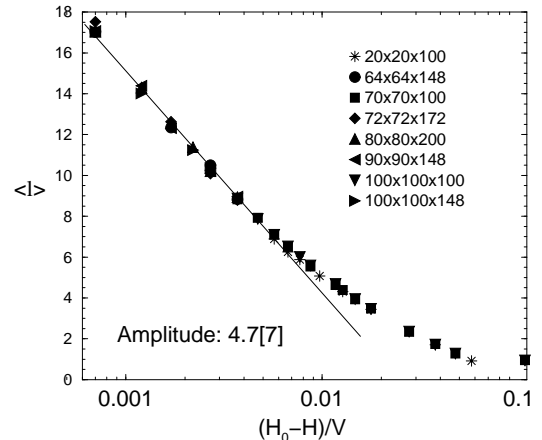


FIG. 6. Position of the interface as estimated from the fit (65) in units of (110) layers vs. $(H - H_0)/V$.

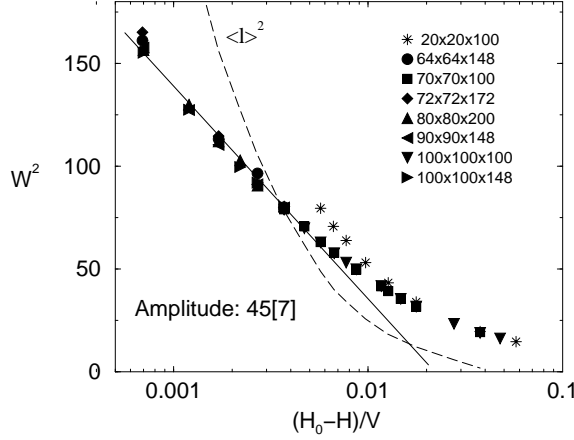


FIG. 7. Squared interfacial width as estimated from the fit (65) in units of (110) layers vs. $(H - H_0)/V$. Long dashed line shows squared interface position $\langle l \rangle^2$ for comparison.

i.e., the width of the interface is smaller than the distance of the interface from the surface. Indeed, Fig. 7 shows that the logarithmic behavior sets in approximately at the value of H where l begins to exceed W . The prefactors of the logarithms in Figs 6 and 7 are predicted to be $(r/2 + \omega/r)\sqrt{2}\xi_b/a_0$ in the case of $\langle l \rangle$ (Fig. 6), and $\pi\omega\xi_b^2/a_0^2$ in the case of W^2 (Fig. 7), where ξ_b is the bulk correlation length, a_0 the lattice constant, a factor $\sqrt{2}$ or 2 accounts for the distance of (110) layers from each other in units of a_0 , and the parameter $r = \max(1, 2\lambda_J/\xi_b)$ depends on the length scale λ_J of composition fluctuations (see the discussion in section IID). We shall see below that the surface data suggest $\beta_1 = r/2 + \omega(1/r - 1/2) = 0.618$. Inserting this result, one derives $4.5[7] < \xi_b/a_0 < 5.4[8]$ from Fig. 6, and $\xi_b/a_0 > 7.8[8]$ from Fig. 7. These values do not agree with each other within in the statistical error; the interfacial width seems to decrease too fast as one moves away from coexistence. Yet the difference seems still acceptable, especially considering how small the region of apparent logarithmic behavior is. It has been observed in other systems [48], that the vicinity of surfaces also affects the intrinsic width W_0 of an interface. Moreover, many non-diverging terms have been neglected in eqns. (39) and (18) which lead to systematic errors if one is not close enough to H_0 . We note that ξ_b seems rather large for a system which is not critical in the bulk. On the other hand, Fig. 5 shows that the bulk order parameter ψ_{23} decreases considerably as one approaches the phase transition point. This observations suggests that a critical point is at least nearby, although preempted by the first order transition from the DO_3 phase to the disordered phase.

Next we consider the profiles of the layer susceptibilities of the order parameter ψ_{23} . They can be determined from the simulation data by use of the fluctuation relations [28]

$$\chi_z = \frac{N_{\text{total}}}{k_B T} \left(\langle \psi(z) \psi_{\text{total}} \rangle - \langle \psi(z) \rangle \langle \psi_{\text{total}} \rangle \right) \quad (66)$$

$$\chi_{zz} = \frac{N_{\text{layer}}}{k_B T} \left(\langle \psi(z)^2 \rangle - \langle \psi(z) \rangle^2 \right), \quad (67)$$

where ψ is the order parameter under consideration, N_{layer} denotes the number of sites in a layer, and N_{total} the total number of sites. Fig. 8 shows that both the layer-bulk susceptibility χ_z and the layer-layer susceptibility χ_{zz} exhibit the expected peak in the vicinity of the interface (eqns. (41) and (22)). The centers of the peaks can be fitted nicely by Gaussians of width ξ_\perp and $\xi_\perp/\sqrt{2}$, respectively, where ξ_\perp is calculated from the width W of the order parameter profile using $\xi_\perp = \sqrt{2/\pi}W$. The wings of the peaks are not Gaussian any more, but asymmetric – the layer susceptibilities are enhanced at the bulk side of the interface, and suppressed at the surface side. Such an asymmetry has been predicted qualitatively for χ_z in eqn. (41), but not for χ_{zz} (cf. eqn. (22)). Even in the case of χ_z , the observed asymmetry is so strong that it cannot be brought into quantitative agree-

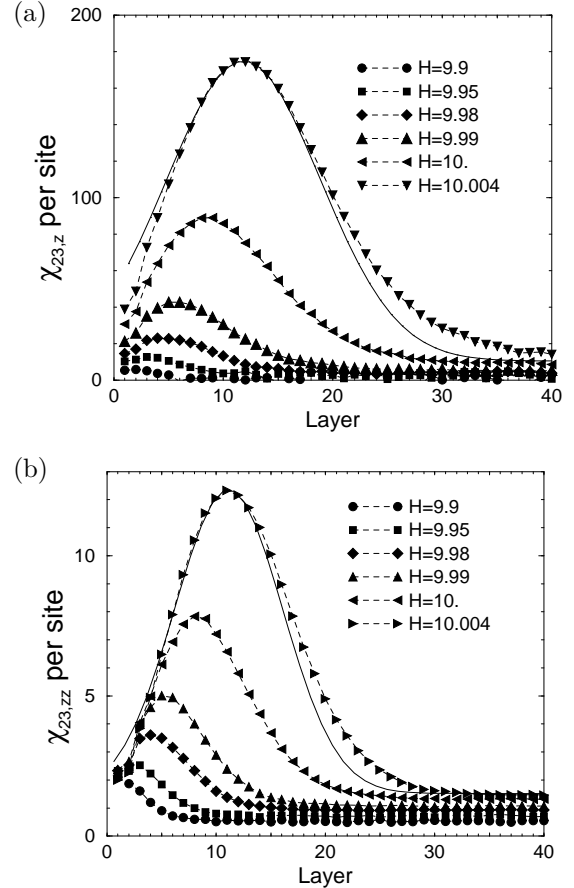


FIG. 8. Profiles of the layer-bulk susceptibility χ_z (a) and the layer-layer susceptibility χ_{zz} (b) per site of the order parameter ψ_{23} in units of $k_B T$, for different fields H in units of V as indicated. Solid line shows the fit of a Gaussian of width (a) $\xi_\perp = (2/\pi)^{1/2}W$ and (b) $\xi_\perp/2^{1/2}$ to the profile corresponding to $H = 10.004$. Zeroth (top) layer is not shown ($\chi(0) \equiv 0$, see text).

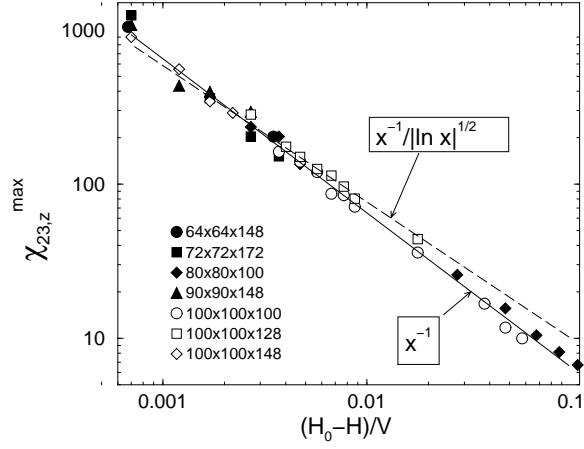


FIG. 9. Maximum of the layer-bulk susceptibility χ_z per site of the order parameter ψ_{23} in units of $k_B T$ vs. $(H_0 - H)/V$ for different system sizes as indicated. Solid line shows a fit to a $(H_0 - H)^{-1}$ behavior, and dashed line the same with logarithmic correction (see text).

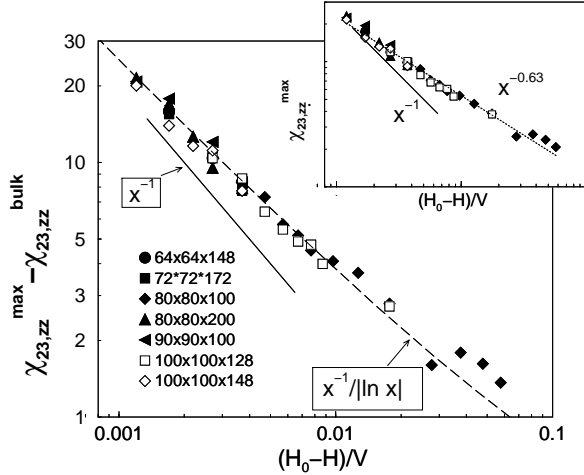


FIG. 10. Maxima of the layer-layer susceptibility χ_{zz} per site of the order parameter ψ_{23} in units of $k_B T$ vs. $(H_0 - H)/V$, for different system sizes as indicated. Inset shows bare data, with a fit to a power law behavior with unknown exponent (dotted line). In the main plot, the bulk contribution to χ_{zz} has been subtracted. Solid line indicates the slope of $(H_0 - H)^{-1}$, and dashed line the whole theoretical prediction including the logarithmic correction.

ment with the theory. We recall that the linear theory approximates the capillary waves of the interface by those of a free interface with some suitable long-wavelength cut-off, *i.e.*, they are taken to be distributed symmetrically about the mean interface position. The failure of the theory to describe the details of the profiles of χ_z and χ_{zz} presumably reflects the fact that the capillary waves are in fact asymmetric. Nevertheless, the main features of the profiles are captured by the theory.

The centers of the peaks are slightly more distant from the surface than $\langle l \rangle$ in Fig. 6, but the difference is not

significant (up to three layers at $(H_0 - H)/V = 0.0007$). According to the theoretical prediction (40) and (42), the heights of the peaks should diverge with $1/(H_0 - H)$ with different logarithmic corrections. Our data are shown in Figs. 9 and 10. The maxima of the layer-bulk susceptibility are best fitted by the simple $1/(H - H_0)$ behavior, which the theory predicts as long as the interfacial width is dominated by the intrinsic width W_0 . In the regime $(H_0 - H)/V < 0.005$, where the capillary wave broadening of the interface becomes significant, the data are also consistent with the logarithmically corrected version $\chi_z^{max} \propto 1/(H_0 - H)\sqrt{|\ln(H_0 - H)|}$ (see Fig. 9).

The analysis of the layer-layer susceptibility is more subtle. From a double logarithmic plot of the raw data, one is tempted to conclude that the predicted $1/(H_0 - H)$ behavior is not valid; the data rather suggest a divergence with a critical exponent 0.63 (Fig. 10, inset). However, since we are not aware of any theoretical explanation which could motivate such an exponent, we believe that the apparent power law behavior over roughly two decades of $(H_0 - H)$ is most likely accidental. Looking at the values of χ_{zz} close to the center of the slab (Fig. 8b)), one recognizes that the contribution of bulk fluctuations to χ_{zz} is significant even close to H_0 . The situation is complicated by the fact that the bulk fluctuations increase considerably in the vicinity of H_0 , although their amplitude does not diverge. Within the crude approximation that the capillary waves of the interface and the bulk fluctuations are uncorrelated, one can subtract the latter as “background”. The thereby corrected data agree reasonably well with the theory, especially when taking into account the logarithmic correction $\chi_{zz}^{max} \propto 1/(H_0 - H)|\ln(H_0 - H)|$ (Fig. 10).

We proceed to study the properties of the system directly at the surface. Figure 11 shows the order parameter $\psi_{23,1}$ in the first layer (recalling that the top (zeroth) layer is discarded) as a function of $(H_0 - H)$ for various

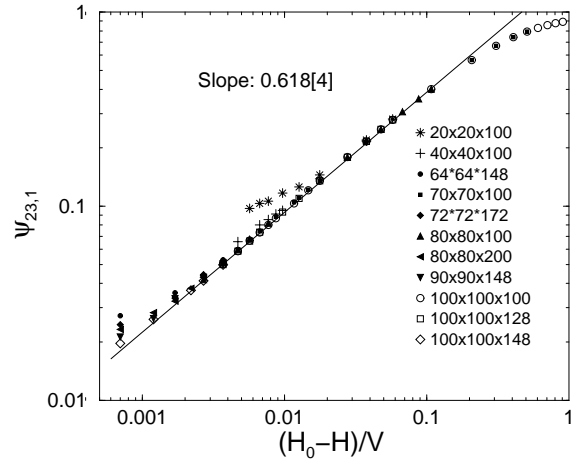


FIG. 11. Order parameter $\psi_{23,1}$ at the surface (first layer) vs. $(H_0 - H)/V$ for different system sizes $L \times L \times D$ as indicated. Solid line indicates power law with the exponent $\beta_1 = 0.618$.

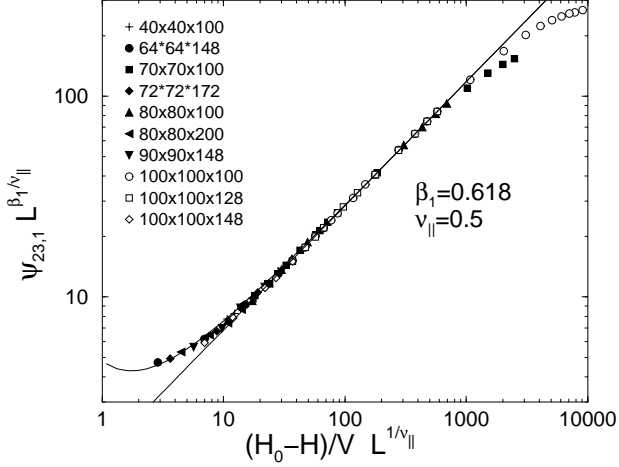


FIG. 12. Finite-size scaled plot of the surface order parameter $\psi_{23,1}$ vs. $(H_0 - H)/V$ for system sizes $L \times L \times D$ as indicated. Data were scaled with exponents $\nu_{||} = 1/2$ and $\beta_1 = 0.618$. Dashed line shows the finite size scaling function predicted by eqn. (51).

system sizes. One notices finite size effects if the dimension L parallel to the interface is small. As long as L is large enough, the data exhibit a power law behavior with the exponent $\beta_1 = 0.618$ [4]. We emphasize that β_1 clearly differs from $1/2$ here. It is close to the value $\beta_1 = 0.64$ found by Schweika *et al* in their simulations of surface induced disorder in fcc-alloys [28]. As discussed in section II D, several factors may lead to such a nonuniversal exponent – capillary wave fluctuations, and/or the presence of a length scale $\lambda_J > \xi_b/2$, which competes with the correlation length ξ_b and would have to be associated with the nonordering composition fluctuations in the case of the symmetry preserving (110) surface. Using eqn. (57), we can derive upper bounds for the capillary parameter, $\omega < 0.236$, and for λ_J , $\lambda_J/\xi_b < 0.618$.

After applying finite size scaling with the exponents β_1 and $\nu_{||} = 1/2$ (cf. eqn. (45)), the data collapse onto a single master curve. The form of the latter can be calculated from eqn. (45),

$$\psi_{23,1} L^{\beta_1/\nu_{||}} \propto \frac{x^{r/2+\omega/r}}{(x+1)^{\omega/2}} e^{2\pi\omega/x} \quad (68)$$

with $x \propto (H_0 - H)L^{1/\nu_{||}}$ and $r = \max(1, 2\lambda_J/\xi_b)$, where the two unknown proportionality constants are fit parameters and $\omega = 0.236$ was used (the result is only very barely sensitive to the choice of ω). Fig. 12 shows that the data agree nicely with the theoretical prediction.

Figure 13 shows the layer-bulk susceptibility at the surface for the order parameter ψ_{23} . According to eqn. (58), it should diverge with the exponent $\gamma_1 = 1 - \beta_1 = 0.382$. Indeed, the fit to our data in the region $(H_0 - H)/V < 0.02$ yields $\gamma_1 = 0.37$ [5]. In the case of the layer-layer susceptibility, the theory (59) predicts $\gamma_{11} = 1 - 2\beta_1 = -0.236$, *i.e.*, χ_{11} does not diverge at the phase transition. In fact, it first increases as H_0 is approached,

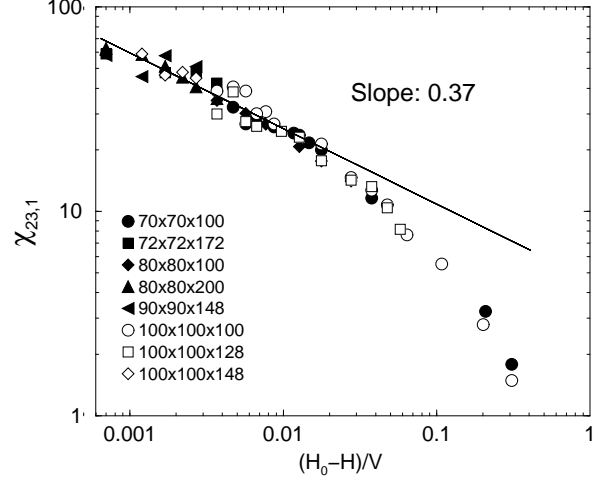


FIG. 13. Surface layer-bulk susceptibility per site of the order parameter ψ_{23} vs. $(H_0 - H)/V$ for different system sizes as indicated. Solid line marks a power law with the exponent $\gamma_1 = 0.37$.

but then decreases for $(H_0 - H)/V < 0.02$ (not shown). The layer-layer susceptibility at the surface here behaves in a similar way as observed by Schweika *et al* in their studies of surface induced disorder at the (111) surface of an fcc-based alloy [28].

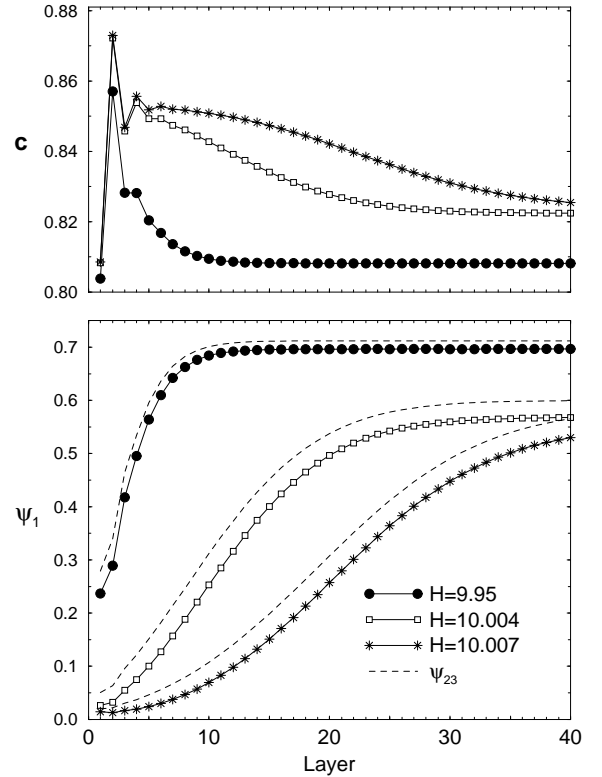


FIG. 14. Profiles of the total composition $c = (\langle S \rangle + 1)/2$ (top) and of the order parameter ψ_1 (bottom) for different fields H in units of V as indicated. Top (zeroth) layer is not shown ($c(0) \equiv 1, \psi_1(0) \equiv (0)$). Thin dashed lines with squares show for comparison the profiles of ψ_{23} from Fig. 5.

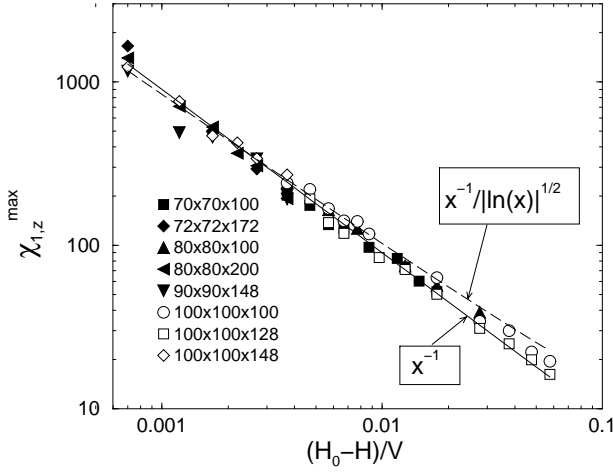


FIG. 15. Maximum of the layer-bulk susceptibility χ_z per site of the order parameter ψ_1 in units of $k_B T$ vs. $(H_0 - H)/V$ for different system sizes as indicated. Solid line shows a fit to a $(H_0 - H)^{-1}$ behavior, and dashed line the same with the appropriate logarithmic correction.

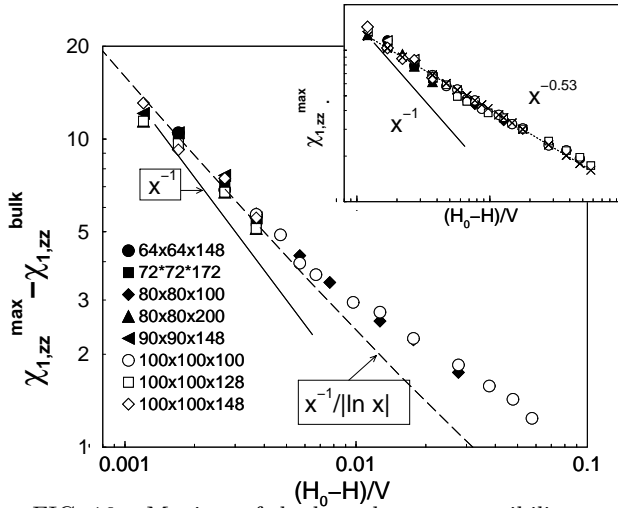


FIG. 16. Maxima of the layer-layer susceptibility χ_{zz} per site of the order parameter ψ_1 minus bulk contribution in units of $k_B T$ vs. $(H_0 - H)/V$, for different system sizes as indicated. Solid line indicates the slope of $(H_0 - H)^{-1}$, and dashed line the whole theoretical prediction including the logarithmic correction. Inset shows bare data, with a fit to a power law behavior (dotted line).

B. (110) Surfaces – B2 order

From the results discussed so far, we conclude that the behavior of the order parameter ψ_{23} can be understood nicely within the effective interface theory of critical wetting. However, we shall see that this holds only in part for the second order parameter, ψ_1 .

Fig. 14 shows profiles of ψ_1 for different fields H . They

resemble those of ψ_{23} , in particular the inflection point of the profiles is located approximately at the same distance from the surface. The upper part of Fig. 14 displays profiles of the total concentration c of A particles (eqn. (63)). They exhibit some characteristic, H -independent oscillations in the first four layers, and the A concentration is slightly enhanced in the disordered region. However, the overall variation is rather small.

The layer susceptibility profiles of the order parameter ψ_1 are qualitatively similar to those of ψ_{23} and not shown here. Fig. 15 demonstrates that the maximum of the layer-bulk susceptibility evolves with the field H as theoretically predicted, $\chi_z^{max} \propto 1/(H_0 - H)\sqrt{|\ln(H_0 - H)|}$. In the case of the layer-layer susceptibility, the agreement with the theoretically expected behavior $(\chi_{zz}^{max} - \chi_{zz}^{bulk}) \propto 1/(H_0 - H)|\ln(H_0 - H)|$ is not quite as convincing, but the data are still consistent with the theory for $(H - H_0)/V < 0.01$ (Fig. 16). Note that the bare values of χ_{zz}^{max} would again rather suggest a power law, $\chi_{zz}^{max} \propto (H_0 - H)^{-0.53}$ (Fig. 16, inset), which is however most likely accidental.

Hence the behavior of the order parameter ψ_1 in the vicinity of the interface is similar to that of the order parameter ψ_{23} and consistent with the theory of critical wetting. The agreement however does not persist when looking right at the surface. Figs. 17 and 18 show how the value of ψ_1 in the first surface layer depends on $(H_0 - H)/V$. A power law behavior is found over one and a half decades of $(H_0 - H)/V$, yet the exponent $\beta_1(\psi_1) = 0.801$ differs from that of $\psi_{23,1}$, $\beta_1(\psi_{23}) = 0.618$ (Fig. 17). Moreover, the data for different system sizes do not collapse if one performs finite size scaling with the exponent $\nu_{\parallel} = 1/2$ (Fig. 18(a)). The collapse is significantly better if one assumes that the parallel correlation length diverges with the exponent $\nu_{\parallel} = 0.7 \pm 0.05$ (Fig. 18 (b)).

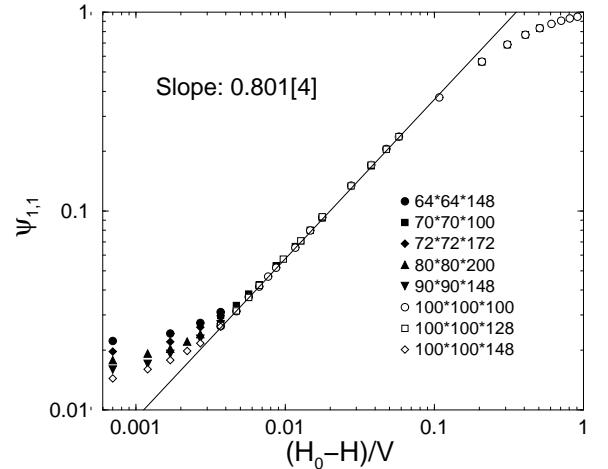


FIG. 17. Order parameter ψ_1 at the surface vs. $(H_0 - H)/V$ for different system sizes $L \times L \times D$ as indicated. Solid line shows power law with the exponent $\beta_1 = 0.801$.

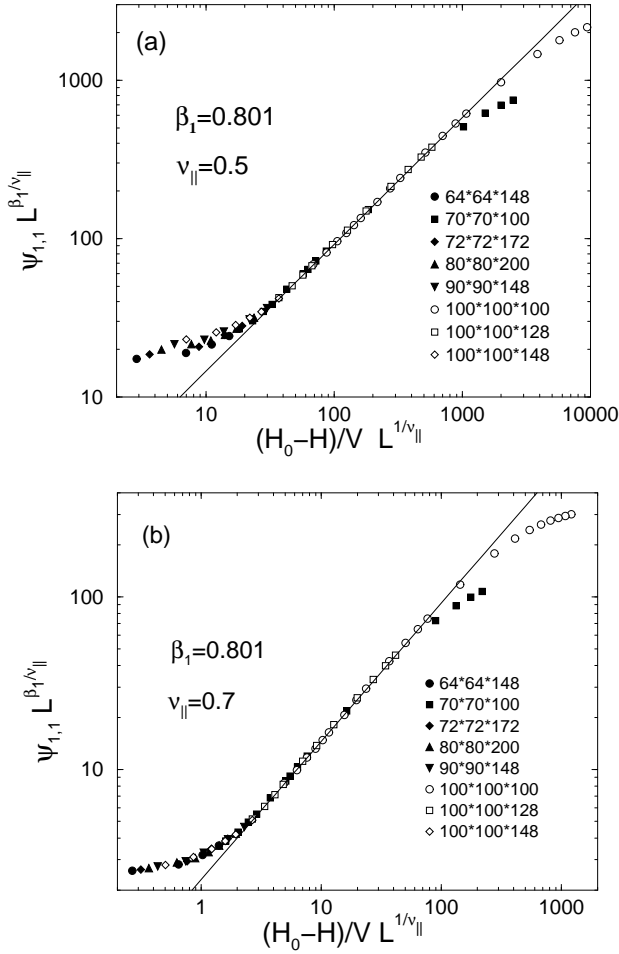


FIG. 18. Finite-size scaled plots of the order parameter ψ_1 at the surface vs. $(H_0 - H)/V$ for system sizes $L \times L \times D$ as indicated. Exponents are $\beta_1 = 0.801$, $\nu_{||} = 0.5$ in (a), and $\nu_{||} = 0.7$ in (b).

We have no explanation for these unexpected findings. The discussion in section II has shown that several surface exponents $\beta_{i,1}$ may be present in a system with several order parameters. Even though we have argued that only the smallest exponent should survive in the asymptotic limit $\mu \rightarrow 0$, the other power law contributions may conceivably still dominate the behavior of certain quantities over a wide range of μ . However, the critical exponent $\nu_{||}$ should in all cases remain invariably $\nu_{||} = 1/2$. Our results seem to indicate that the behavior of the order parameter ψ_1 at the surface is governed by a length scale, which differs from that given of the interfacial fluctuations, but which nonetheless diverges as H_0 is approached. Note that $\nu_{||} \approx 0.7$ is close to the exponent $\nu = 0.63$ with which the bulk correlation length diverges at an Ising type transition in three dimensions. Likewise, the exponent $\beta_1 = 0.801$ found here resembles the surface critical exponent of the ordinary transition, $\beta_1 \sim 0.8$ [49,50]. One might thus suspect that ψ_1 in the disordered surface layer becomes critical at H_0 . However, such a co-

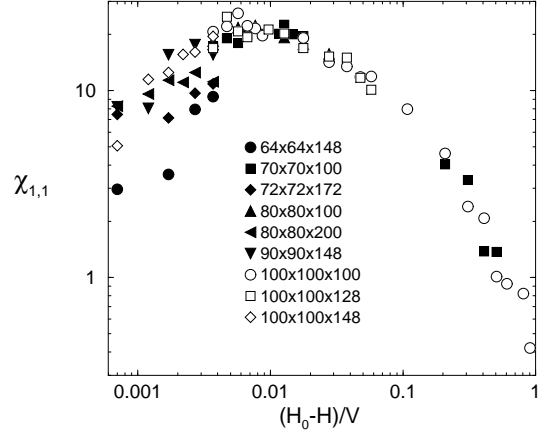


FIG. 19. Surface layer-bulk susceptibility per site of the order parameter ψ_1 vs. $(H_0 - H)/V$ for different system sizes as indicated.

incidence would seem rather surprising. Furthermore, we have noted earlier that the combination $\psi_2\psi_3$ acts as an ordering field on ψ_1 , hence ψ_1 cannot become critical as long as ψ_{23} is not strictly zero.

Figure 19 shows the layer-bulk susceptibility at the surface as a function of $(H_0 - H)/V$. It decreases as H_0 is approached, hence the scaling relation $\beta_1 + \gamma_1 = 1$ is obviously not met for the order parameter $\psi_{1,1}$.

C. (100) Surfaces

Finally, we turn to the discussion of (100) surfaces. As already mentioned earlier, (100) surfaces break the symmetry with respect to the order parameter ψ_1 , an ordering surface field coupling to this order parameter is allowed and thus usually present [11,14]. This field is often closely related to surface segregation [11,40]. In our case, the excess component A of the DO_3 segregates in the surface layer and induces a staggered concentration field in the layers underneath, which is equivalent to ψ_1 ordering.

This is demonstrated in Fig. 20. The order parameters and the composition c are defined based on the sublattice occupancies on two subsequent layers of distance $a_0/2$, starting from the first layer underneath the surface. The top layer is again disregarded, since it is entirely filled with A or $S \equiv 1$. The profiles of ψ_1 clearly display the signature of an additional ordering tendency at the surface, which in fact reverses the sign of ψ_1 in the top layers. However, the effect is rather weak and does not influence the system significantly deeper in the bulk. The profiles can be analyzed like those at the (110) surface, and mean interface positions and mean interfacial widths can be extracted to yield figures very similar to Figs. 6 and 7. The amplitudes of the logarithmic divergences can again be used to estimate the bulk correlation length ξ_b . From the mean interface position, one

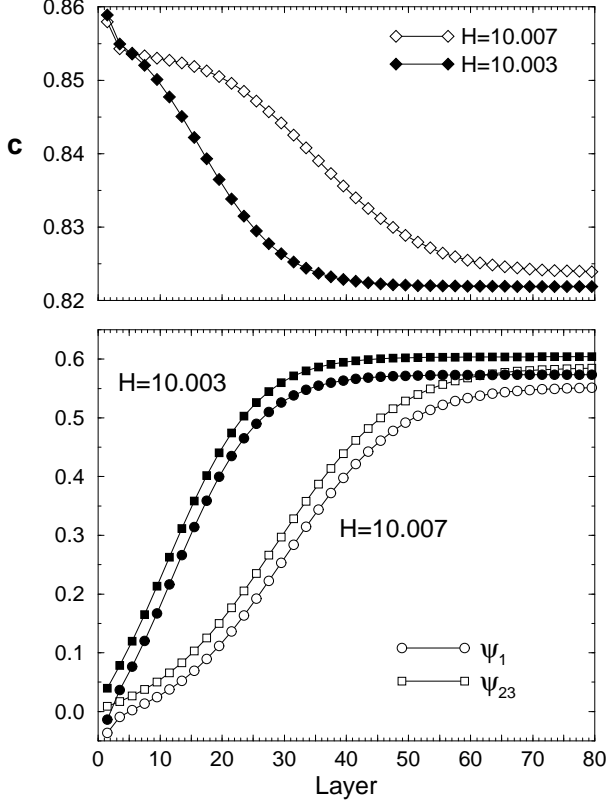


FIG. 20. Profiles of the total concentration of A (top, diamonds), of the order parameters ψ_1 (bottom, circles) and ψ_{23} (bottom, squares) at $H = 10.003$ (filled symbols) and at $H = 10.007$ (open symbols). Zeroth (top) layer is not shown.

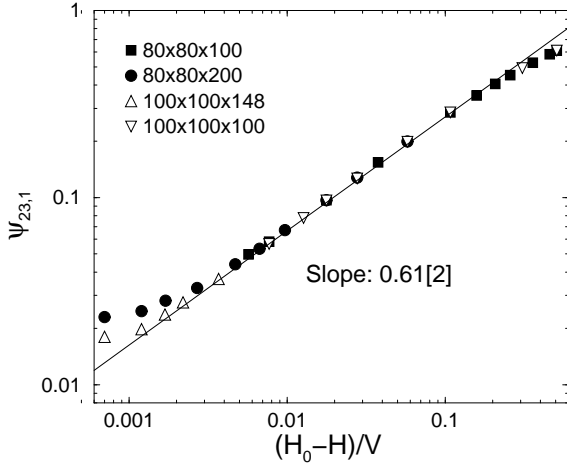


FIG. 21. Order parameter ψ_{23} at the surface vs. $(H_0 - H)/V$ for different system sizes $L \times L \times D$ as indicated. Solid line shows power law with the exponent $\beta_1 = 0.61$.

calculates $4.9[7] < \xi_b/a_0 < 5.8[8]$, and from the interfacial width, $\xi_b/a_0 > 7.5[9]$, in agreement with the values obtained for the (110) surface. Likewise, the study of the layer susceptibilities at the interface does not offer

new surprises. The maxima of the layer-bulk susceptibilities for both ψ_1 and ψ_{23} grow according to a power law $\chi_z \propto (H_0 - H)^{-1}$. The layer-layer susceptibility in the interfacial region seems to grow with a different exponent (~ 0.6 like in the case of the (110) surface), yet after subtracting the “background” the data are also consistent with the theoretically expected behavior. Last, we study how the surface value of the order parameter ψ_{23} evolves as the transition H_0 is approached. Fig. 21 shows that it vanishes according to a power law with the exponent $\beta_1 = 0.61[2]$, which is within the error the same exponent as in the case of the (110) surface. As far as the surface behavior of ψ_{23} is concerned, the (100) and the (110) surface are thus basically equivalent. The weak ordering tendency of ψ_1 has an at most slightly perturbing effect on the profiles of ψ_{23} .

V. SUMMARY AND OUTLOOK

We have presented an extensive Monte Carlo study of surface induced disorder in a simple spin lattice model for bcc-based binary alloys. Our work complements earlier Monte Carlo simulations of Schweika *et al* [28], who have studied surface induced disorder in fcc-based alloys within a similar model. Like these authors, we observe critical wetting behavior with nonuniversal exponents. We have discussed our results in terms of an effective interface model designed to describe a system with several order parameters. In such a complex material, nonuniversal exponents may result both from fluctuation effects and from a competition of length scales.

Due to the complicated order parameter structure in our system, however, our data could not fully be explained within a theory which traces everything back to the properties of a single interface between a disordered and an ordered phase. The theory provides a satisfactory picture for the behavior of the order parameter describing the DO₃ ordering, ψ_{23} , and in general for the structure in the interfacial region. However, it fails to predict the behavior of the order parameter of B2 ordering, ψ_1 , directly at the surface. Our data thus indicate that the fluctuations of ψ_1 at the surface require special treatment. Parry and coworkers [34,51] have recently suggested an approach to a theory of wetting based on an effective interface Hamiltonian with two “interfaces”, the usual one separating the phase adsorbed at the surface and the bulk phase, and a second one which accounts in an effective way for the fluctuations directly at the surface. Our problem seems to call for such an approach. Unfortunately, we are far from understanding even the constituting elements, the fluctuations of ψ_1 at the wall. We seem to observe a coupling between critical wetting and some kind of surface critical behavior of ψ_1 , the origin of which is unclear.

Hence already our simple, highly idealized model exhibits a complex and rather intriguing wetting behav-

ior. In real alloys, numerous additional complications are present which will lead to an even richer and more interesting phenomenology. For example, long range interactions are known to influence wetting transitions significantly. The effect of van-der-Waals forces on wetting has been investigated in detail [1]. Van-der-Waals forces are important in liquid-vapour systems or binary fluids, but presumably irrelevant in alloys. Instead, elastic interactions caused by lattice distortions presumably play an important role.

Furthermore, real surfaces are never ideally smooth, but have steps and islands. We have seen that the orientation of the surface affects the surface ordering. In our study, we did not observe dramatic differences between the (110) surface and the (100) surface. Nevertheless, we expect that the influence of the surface orientation on the wetting behavior can be quite substantial, *e.g.*, in situations with strong surface segregation, or if surface orientations are involved which also break the symmetry with respect to the DO_3 order (*e.g.*, the (111) surface). Likewise, we can expect that steps and islands will affect the ordering and the wetting properties of the alloy. It is well known in general that the wetting behavior on corrugated or rough surfaces differs from that on smooth surfaces [52–54]. In addition, even a few steps or islands on an otherwise smooth, but symmetry breaking surface of an alloy can have a dramatic effect on the ordering behavior, since every step changes the sign of the ordering surface field.

ACKNOWLEDGMENTS

We wish to thank M. Müller and A. Werner for helpful discussions. F.F.H. acknowledges financial support from the Graduiertenförderung of the Land Rheinland Pfalz, and F.S. has been supported from the Deutsche Forschungsgemeinschaft through the Heisenberg program.

-
- [1] for reviews on wetting see, *e.g.*, P. G. de Gennes, Rev. Mod. Phys. **57**, 827 (1985); S. Dietrich in *Phase Transitions and Critical Phenomena*, C. Domb and J.L. Lebowitz eds (Academic Press, New York, 1988), Vol. 12; M. Schick in *Les Houches, Session XLVIII – Liquids at Interfaces*, J. Charvolin, J. F. Joanny, and J. Zinn-Justin eds (Elsevier Science Publishers B.V., 1990).
 - [2] for short overviews on recent progress see, *e.g.*, E. M. Blokhuis and B. Widom, Curr. Opns in Coll. Interf. Science **1**, 424 (1996); G. H. Findenegg and S. Herminghaus, Curr. Opns in Coll. Interf. Science **2**, 301 (1997).
 - [3] K. Ragil, J. Meunier, D. Broseta, J. O. Indekeu, and D. Bonn, Phys. Rev. Lett. **77**, 1532 (1996).
 - [4] D. Ross, D. Bonn, and J. Meunier, Nature **400**, 737 (1999); D. Ross, D. Bonn, and J. Meunier, preprint 1999.
 - [5] R. Lipowsky, Phys. Rev. Lett. **49**, 1575 (1982); R. Lipowsky and W. Speth, Phys. Rev. B **28**, 3983 (1983).
 - [6] D. M. Kroll and R. Lipowsky, Phys. Rev. B **28**, 6435 (1983).
 - [7] R. Lipowsky, J. Appl. Phys. **55**, 2485 (1984).
 - [8] H. Dosch, *Critical Phenomena at Surfaces and Interfaces (Evanescent X-ray and Neutron Scattering)*, Springer Tracts in Modern Physics Vol 126 (Springer, Berlin, 1992).
 - [9] J. W. Cahn, J. Chem. Phys. **66**, 3667 (1977).
 - [10] Under certain, rather unusual circumstances, the critical wetting point could be approached on a complete wetting path, however (see section II C).
 - [11] F. Schmid, Zeitschr. f. Phys. **B 91**, 77 (1993).
 - [12] F. Schmid, in *Stability of Materials*, p 173, A. Gonis *et al* eds., (Plenum Press, New York, 1996).
 - [13] S. Krimmel, W. Donner, B. Nickel, and H. Dosch, Phys. Rev. Lett. **78**, 3880 (1997).
 - [14] A. Drewitz, R. Leidl, T. W. Burkhardt, and H. W. Diehl, Phys. Rev. Lett. **78**, 1090 (1997); R. Leidl and H. W. Diehl, Phys. Rev. B **57**, 1908 (1998); R. Leidl, A. Drewitz, and H. W. Diehl, Intl. Journal of Thermophysics **19**, 1219 (1998).
 - [15] P. J. Upton, D. Abraham, to be published.
 - [16] W. Helbing, B. Dünweg, K. Binder, and D. P. Landau, Z. Phys. B **80**, 401 (1990).
 - [17] D. M. Kroll, G. Gompper, Phys. Rev. B **36**, 7078 (1987);
 - [18] G. Gompper, D. M. Kroll, Phys. Rev. B **38**, 459 (1988).
 - [19] L. Mailänder, H. Dosch, J. Peisl, R.L. Johnson, Phys. Rev. Lett. **64**, 2527 (1990).
 - [20] W. Schweika, K. Binder, and D. P. Landau, Phys. Rev. Lett. **65**, 3321 (1990).
 - [21] W. Schweika, D.P. Landau, in *Computer Simulation Studies in Condensed-Matter Physics X*, P. 186 (1997).
 - [22] V. S. Sundaram, B. Farrell, R. S. Alben, and W. D. Robertson, Phys. Rev. Lett. **31**, 1136 (1973).
 - [23] E. G. McRae and R. A. Malic, Surf. Sci. **148**, 551 (1984).
 - [24] S. F. Alvarado, M. Campagna, A. Fattah, and W. Uelhoff, Z. Phys. B **66**, 103 (1987).
 - [25] H. Dosch, L. Mailänder, A. Lied, J. Peisl, F. Grey, R. L. Johnson, and S. Krummacher, Phys. Rev. Lett. **60**, 2382 (1988); H. Dosch, L. Mailänder, H. Reichert, J. Peisl, and R. L. Johnson, Phys. Rev. B **43**, 13172 (1991).
 - [26] Ch. Ricolleau, A. Loiseau, F. Ducastelle, and R. Caudron, Phys. Rev. Lett. **68**, 3591 (1992).
 - [27] V. S. Sundaram, R. S. Alben, and W. D. Robertson, Surf. Sci. **46**, 653 (1974).
 - [28] W. Schweika, D.P. Landau, and K. Binder, Phys. Rev. B **53**, 8937 (1996).
 - [29] K. Binder, D. P. Landau, and D. M. Kroll, Phys. Rev. Lett. **56**, 2272 (1986); K. Binder and D. P. Landau, Phys. Rev. B **37**, 1745 (1988); K. Binder, D. P. Landau, and S. Wansleben, Phys. Rev. B **40**, 6971 (1989).
 - [30] E. Brézin, B. I. Halperin, and S. Leibler, Phys. Rev. Lett. **50**, 1387 (1983).
 - [31] D. S. Fisher and D. A. Huse, Phys. Rev. B **32**, 247 (1985).
 - [32] M. E. Fisher and A. J. Jin, Phys. Rev. Lett. **69**, 792 (1992).

- [33] C. J. Boulter, Phys. Rev. Lett. **79**, 1897 (1997).
- [34] P. S. Swain and A. O. Parry, Europhys. Lett. **37**, 207 (1997).
- [35] E.H. Hauge, Phys. Rev. B **33**, 3322 (1986).
- [36] R. Lipowsky, D. M. Kroll, and R. K. P. Zia, Phys. Rev. B **27**, 4499 (1983).
- [37] For a review see M. E. Fisher in *Statistical Mechanics of Membranes and Surfaces*, D. R. Nelson, T. Piran, R. B. Weinberg eds. (World Scientific, Singapore, 1989).
- [38] R. Lipowsky and M. E. Fisher, Phys. Rev. B **36**, 2126 (1987).
- [39] D. Bedeaux and J. D. Weeks, J. Chem. Phys. **82**, 972 (1985).
- [40] F. Schmid and K. Binder, Phys. Rev. B **46**, 13553 (1992); F. Schmid, K. Binder, Phys. Rev. B **46**, 13565 (1992).
- [41] A. Werner, F. Schmid, M. Müller, and K. Binder, J. Chem. Phys. **107**, 8175 (1997).
- [42] O. Kubaschewski in *Iron – Binary Phase Diagrams*, p 5, (Springer, Berlin 1982).
- [43] B. Dünweg and K. Binder, Phys. Rev. B **36**, 6935 (1987).
- [44] For details see F. F. Haas, Dissertation (Johannes Gutenberg Universität Mainz 1998).
- [45] G. Bhanot, D. Duke, and R. Salvator, J. Stat. Phys. **44**, 985 (1986).
- [46] Our multispin code differs from the one described in [45] in that we could not make use of bit operations, unfortunately, due to the complicated nature of the interactions in our model.
- [47] K. Binder, Z. Phys. B **45**, 61 (1981).
- [48] K. Binder, M. Müller, F. Schmid, A. Werner, J. Stat. Phys. **95**, 1045 (1999).
- [49] H. W. Diehl, in *Phase Transitions and Critical Phenomena*, Vol. 8, C. Domb and J. Lebowitz eds. (Academic, London, 1983).
- [50] D. P. Landau and K. Binder, Phys. Rev. B **41**, 4633 (1990).
- [51] C. J. Boulter and A. O. Parry, Phys. Rev. Lett. **74**, 3403 (1995); A. O. Parry and C. J. Boulter, Physica A **218**, 77 (1995); C. J. Boulter and A. O. Parry, Physica A **218**, 109 (1995); A. O. Parry, J. Phys.: Cond. Matt. **8**, 10761 (1996).
- [52] C. Borgs, J. De Coninck, R. Kotecký, and M. Zinque, Phys. Rev. Lett. **74**, 2292 (1995);
- [53] R. R. Netz and D. Andelman, Phys. Rev. E **55**, 687 (1997).
- [54] A. O. Parry, P. S. Swain, and J. A. Fox, J. Phys.: Cond. Matt. **8**, L659 (1996); P. S. Swain and A. O. Parry, J. Phys. A: Math. Gen. **30**, 4597 (1997); P. S. Swain and A. O. Parry, Eur. Phys. J. B **4**, 459 (1998).